Structural and dynamical properties of a new family of solid solutions: $BaMn_{1-x}Zn_xF_4$

1996 J. Phys.: Condens. Matter 8 4993

(http://iopscience.iop.org/0953-8984/8/27/010)

J. Phys.: Condens. Matter **8** (1996) 4993–5005. Printed in the UK

Structural and dynamical properties of a new family of solid solutions: $BaMn_{1-x}Zn_xF_4$

H N Bordallo†, R Almairac†, A Bulou‡ and J Nouet‡

† Groupe de Dynamique des Phases Condensées, UMR 5581, Université Montpellier II, cc 26, 34095, Montpellier Cédex 05, France

‡ Laboratoire de Physique de l'Etat Condensé, URA CNRS 807, Université du Maine, 72017, Le Mans Cédex, France

Received 14 December 1995, in final form 19 February 1996

Abstract. The new solid solutions $BaMn_{1-x}Zn_xF_4$ have been investigated by different experimental methods in the temperature range 10 K–300 K. X-ray and calorimetric measurements show that the incommensurate phase characteristic of $BaMnF_4$ is also observed for $x \leqslant 0.25$. Raman spectra were obtained for $BaMn_{0.5}Zn_{0.5}F_4$ and $BaMn_{0.25}Zn_{0.75}F_4$. Two low-frequency, temperature-dependent bands were observed over the whole temperature range investigated. These results are discussed in connection with structural disorder and the presence of precursor effects of an incommensurate phase transition.

1. Introduction

Crystals of $BaMnF_4$ and $BaZnF_4$ are isomorphous and have polar symmetry (space group $A2_1am$, C_{2v}^{12}) [1, 2]. New interest in this family of materials arose recently in the field of ferroelectric semiconductor heterostructures [3].

In the case of $BaMnF_4$ an incommensurate phase transition has been observed [4] below $T_i \approx 250$ K. Extensive work has been done on this compound because of its unusual structural, magnetic and electrical properties [5–9]. Much of this work has already been summarized by Scott in a lengthy review [10]. On the other hand quite a few investigations have been undertaken on $BaZnF_4$ [11–12], but why it exhibits a different behaviour has not yet been elucidated.

Recently we have reported Raman measurements on $BaZnF_4$ crystals [13]. On the basis of these results we suggested a breaking of the $C_{2v}(a, b, c)$ selection rules due either to a phase transition or to structural disorder. This led us to perform a study by x-ray scattering [14] which showed that no phase transition occurs. On the other hand, rod-like diffuse intensities were observed at room temperature and were interpreted as the occurrence of 2D dynamical clusters. In this interpretation some order occurs in (a, c) planes, the planes in which the ZnF_6 octahedra are rigidly linked together, but no order occurs between neighbouring planes, in the ***b***-direction. It has been shown that these 2D clusters can be viewed as precursors of an instability of the same type as the instability giving rise to the incommensurate phase in $BaMnF_4$.

The aim of the present paper is to describe the evolution of these 2D dynamical clusters as a function of the chemical substitution and temperature in $BaMn_{1-x}Zn_xF_4$ solid solutions.

X-ray and calorimetric measurements which were performed in order to obtain the phase diagram of these compounds are reported in section 2. In section 3 the Raman

0953-8984/96/274993+13$19.50

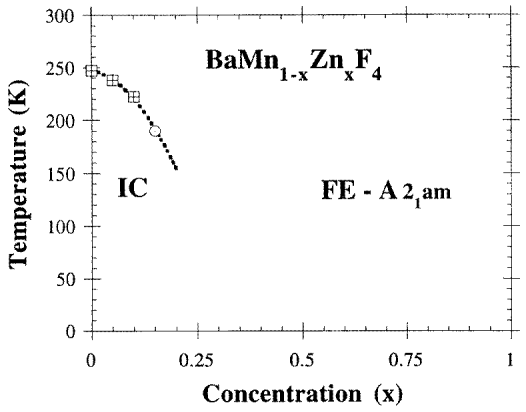

Figure 1. A partial phase diagram of the $BaMn_{1-x}Zn_xF_4$ solid solution. The open circle corresponds to the x-ray measurements.

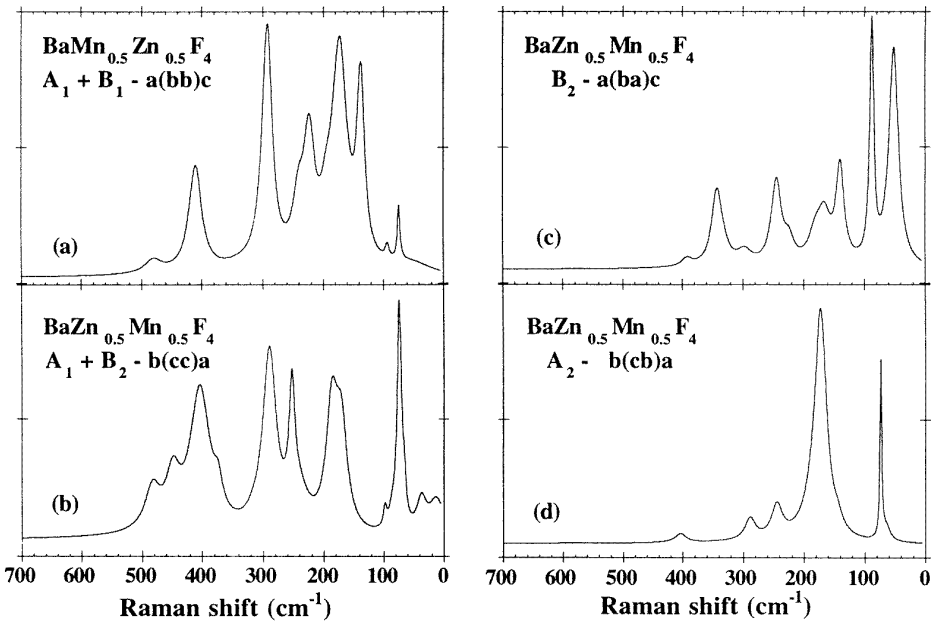

Figure 2. Raman spectra obtained at room temperature for $BaMn_{0.5}Zn_{0.5}F_4$: (a) $a(bb)c$, (b) $b(cc)a$, (c) $a(ba)c$ and (d) $b(cb)a$.

spectra obtained as functions of concentration and temperature are presented. All of the results are summarized and discussed in section 4.

2. The phase diagram

Single crystals of $BaMn_{1-x}Zn_xF_4$ with various compositions were synthesized by G Niesseron at the Laboratoire de Physique de l'Etat Condensé by the Bridgman–Stockbarger

Table 1. Frequencies (cm^{-1}) of the modes (*aa*), (*bb*) and (*cc*) for the solid solution $BaMn_{1-x}Zn_xF_4$, $x = 0$ [15–17], 0.5, 0.75 and 1 [13], at room temperature. The modes are: S = strong, m = medium or w = weak. The other abbreviations indicate a shoulder (sh) or a contamination (c).

A_1–$b(aa)c$			$A_1 + B_1$–$a(bb)c$				$A_1 + B_2$–$b(cc)a$			
$x = 0$	$x = 0.75$	$x = 1$	$x = 0$	$x = 0.5$	$x = 0.75$	$x = 1$	$x = 0$	$x = 0.5$	$x = 0.75$	$x = 1$
—	—	—	—	—	—	—	0^{w}	0^{w}	0^{w}	0^{w}
—	—	—	—	—	—	—	—	15^{m}	—	—
45^{sh}	49^{sh}	—	—	—	—	—	—	37^{m}	40^{m}	48^{w}
—	—	—	—	53^{c}	52^{c}	52^{c}	—	—	—	—
—	—	—	—	—	—	—	—	67^{m}	63^{m}	62^{m}
72^{m}	73^{m}	72^{m}	71^{m}	74^{m}	73^{m}	73^{m}	74^{S}	74^{S}	75^{S}	75^{m}
—	—	—	—	—	—	—	—	—	—	86^{sh}
93^{S}	94^{S}	94^{S}	93^{m}	93^{w}	—	96^{w}	96^{w}	97^{w}	98^{w}	100^{w}
—	—	—	—	—	—	—	—	—	—	113^{c}
124^{m}	133^{m}	136^{m}	130^{S}	137^{S}	137^{m}	139^{m}	—	—	—	—
—	—	—	—	—	—	—	135^{w}	—	—	144^{sh}
145^{w}	141^{w}	166^{w}	—	—	164^{S}	166^{S}	176^{S}	170^{m}	169^{m}	169^{m}
—	173^{w}	179^{w}	161^{S}	172^{S}	179^{S}	176^{S}	—	—	—	—
—	—	—	—	—	—	185^{S}	194^{m}	191^{m}	191^{m}	188^{m}
196^{w}	195^{w}	195^{w}	196^{m}	195^{sh}	—	—	—	—	—	—
—	—	—	—	—	—	—	—	—	—	204^{m}
—	—	—	229^{m}	223^{m}	235^{S}	231^{S}	—	—	—	—
242^{w}	245^{w}	249^{w}	240^{m}	240^{sh}	—	247^{S}	—	—	—	248^{w}
—	—	—	—	—	—	—	250^{m}	253^{m}	253^{S}	259^{m}
264^{w}	269^{w}	275^{w}	—	—	—	278^{sh}	—	—	—	—
—	289^{w}	295^{w}	287^{S}	292^{S}	294^{S}	295^{S}	288^{S}	289^{S}	293^{S}	294^{m}
—	—	—	—	—	—	—	—	—	—	—
—	—	—	—	—	—	—	—	—	324^{sh}	331^{w}
—	—	—	—	—	—	—	—	—	—	—
—	—	—	—	—	—	—	366^{m}	374^{m}	377^{w}	379^{w}
—	—	—	—	—	—	—	380^{m}	403^{S}	410^{S}	412^{S}
402^{w}	418^{S}	426^{S}	399^{m}	410^{S}	419^{S}	427^{S}	396^{m}	—	423^{S}	428^{S}
—	—	—	—	—	—	—	435^{m}	448^{m}	454^{m}	461^{m}
—	495^{w}	510^{w}	—	480^{m}	487^{m}	510^{w}	—	482^{m}	489^{w}	497^{m}

method.

In order to check the space group, Weissenberg photographs were taken at room temperature and at 120 K for the composition $x = 0.50$. The only systematic absences correspond to $k + l = 2n + 1$ for general reflections hkl, and to $h = 2n + 1$ for $h0l$, reproducing the selection rules of the space group $A2_1am$ (C_{2v}^{12}).

X-ray experiments, performed using a home-made diffractometer (see [14] for details), and differential scanning calorimetry measurements, performed with a Perkin–Elmer DSC4 apparatus, permitted us to draw a partial phase diagram of $BaMn_{1-x}Zn_xF_4$.

Because of the incommensurate phase below T_i observed for the solid solution $BaMn_{0.85}Zn_{0.15}F_4$, several satellite reflections at $\boldsymbol{q} = (\delta, 0.5, 0.5)$ characteristic of a modulation wave in the $\boldsymbol{a}$-direction appear in reciprocal space. Measuring the intensity of one of these reflections as a function of temperature gives $T_i \approx 190$ K.

For $x = 0, 0.05$ and 0.10 only calorimetric measurements have been performed. The phase diagram is shown in figure 1. We note that the incommensurate transition is observed for $x \leqslant 0.25$.

Table 2. Frequencies (cm^{-1}) of the modes (ab), (ac) and (bc) for the solid solution $BaMn_{1-x}Zn_xF_4$, $x = 0$ [15–17], 0.5, 0.75 and 1 [13], at room temperature. The modes are: S = strong, m = medium or w = weak. The other abbreviations indicate a shoulder (sh) or a contamination (c).

B_2–$a(ba)c$				$B_1 + B_2$–$c(ac)b$			A_2–$b(cb)a$			
$x = 0$	$x = 0.5$	$x = 0.75$	$x = 1$	$x = 0$	$x = 0.75$	$x = 1$	$x = 0$	$x = 0.5$	$x = 0.75$	$x = 1$
—	—	—	—	—	—	—	—	—	—	—
—	—	—	—	—	—	—	—	—	—	—
—	—	—	—	—	—	—	—	—	—	—
50^{sh}	51^{S}	51^{S}	52^{S}	—	—	—	—	—	—	—
62^{S}	—	—	—	—	—	—	—	61^{c}	62^{c}	62^{c}
—	—	—	—	—	—	—	71^{m}	75^{m}	76^{m}	76^{m}
—	—	—	—	—	—	—	—	—	—	—
85^{S}	87^{S}	89^{S}	91^{S}	—	93^{c}	—	—	—	95^{c}—	
—	—	—	—	115^{w}	112^{m}	112^{m}	—	—	—	115^{w}
—	—	—	—	—	—	—	—	—	—	—
142^{m}	140^{m}	142^{m}	144^{m}	—	—	—	—	144^{c}	—	—
158^{m}	165^{w}	164^{w}	168^{w}	—	—	—	—	—	—	—
—	—	—	—	—	180^{S}	—	—	—	—	—
175^{w}	180^{w}	181^{w}	186^{w}	—	—	—	160^{S}	172^{S}	178^{S}	181^{S}
—	—	—	—	—	—	—	—	—	—	—
—	—	—	—	220^{sh}	215^{m}	207^{m}	—	—	—	204^{w}
230^{w}	226^{w}	231^{w}	232^{w}	—	—	—	—	—	—	—
238^{w}	244^{m}	248^{w}	251^{w}	236^{S}	246^{S}	252^{S}	—	244^{c}	247^{c}	253^{c}
—	—	—	—	—	—	—	—	—	—	—
—	—	—	—	—	—	—	—	—	—	—
—	—	—	—	—	292^{sh}	—	—	289^{w}	292^{w}	292^{w}
—	297^{w}	300^{w}	304^{w}	—	—	—	—	—	—	—
—	—	—	—	—	—	—	—	—	—	—
320^{m}	342^{m}	350^{m}	359^{m}	—	—	—	—	—	—	—
—	—	—	—	—	—	—	—	—	—	—
—	392^{w}	403^{w}	405^{w}	—	—	—	—	—	—	—
—	—	—	429^{c}	—	—	—	—	404^{w}	427^{w}	427^{w}
—	—	—	—	—	—	—	—	—	—	—
—	—	—	—	—	—	—	—	—	—	—

3. Raman results

Raman measurements were carried out on samples cut and polished with faces oriented normal to the $\boldsymbol{a}$, $\boldsymbol{b}$ and $\boldsymbol{c}$ crystal axes, after orientation by x-ray techniques. For the excitation of the sample the 488 nm line of a Coherent Innova 90 Ar-ion laser was used, with a maximum power of 300 mW. A triple-monochromator DILOR Z24 Raman spectrometer was used to analyse the light scattered in the classical 90° geometry, with a typical resolution of 2 cm^{-1}.

3.1. Raman spectra as functions of the concentration at $T = 300$ K

The Raman spectra obtained at room temperature for $BaMn_{0.5}Zn_{0.5}F_4$ and $BaMn_{0.25}Zn_{0.75}F_4$ for different configurations are presented in figures 2 and 3.

Tables 1 and 2 give the mode frequencies for different symmetries, whose values resulted from a fitting procedure applied to the data with an appropriate number of Lorentzian components. The frequencies of the modes of pure compounds are also reported [13, 15–17].

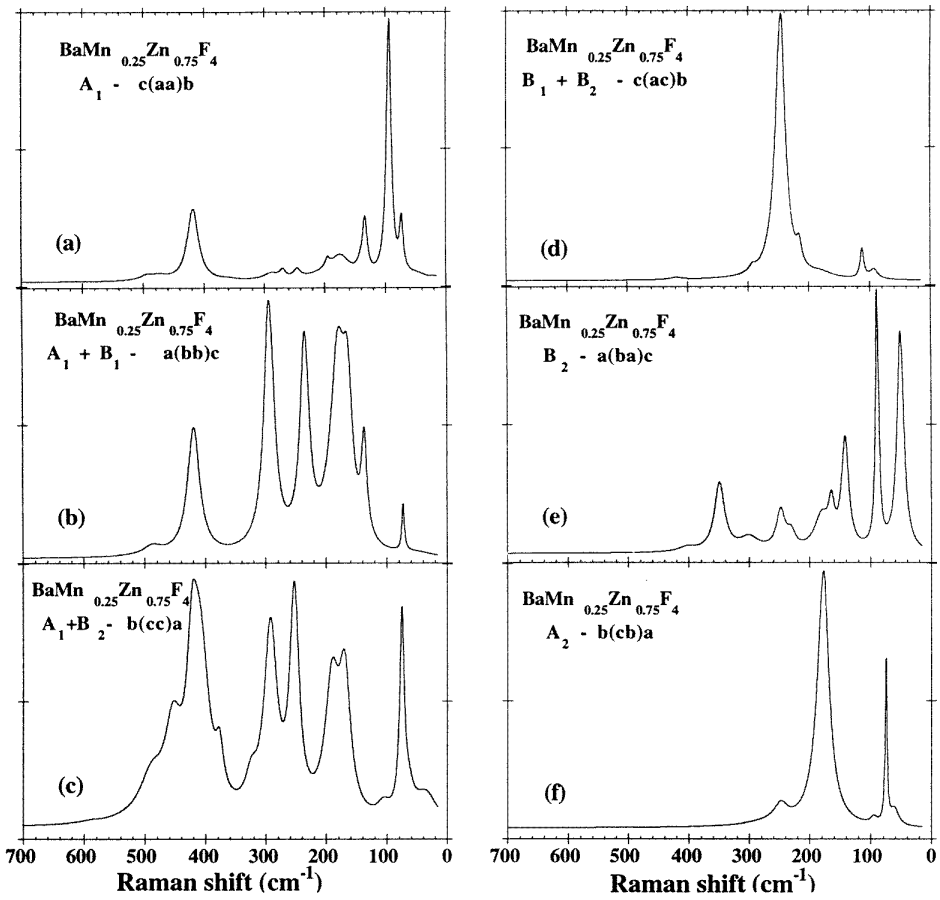

Figure 3. Raman spectra obtained at room temperature for $BaMn_{0.25}Zn_{0.75}F_4$: (a) $c(aa)b$, (b) $a(bb)c$, (c) $b(cc)a$, (d) $c(ac)b$, (e) $a(ba)c$ and (f) $b(cb)a$.

At first sight these spectra present strong similarities for all x-values. However, a detailed comparative analysis of the present results and those for $BaZnF_4$ call for the following remarks.

(1) In the $a(bb)c$ and $a(ba)c$ configurations there is a modification of the relative intensities of the modes located between 130 and 250 cm^{-1} and between 200 and 260 cm^{-1}, respectively. In the totally symmetric configuration some modes are not separated because of their larger widths.

(2) In the (cc) spectra only one group of modes is observed in the region located between 140 and 205 cm^{-1}; a modification of the relative intensities of the modes is observed between 290 and 520 cm^{-1}.

A more remarkable point concerns the responses observed in the lower-frequency range between 5 and 50 cm^{-1}. A detailed analysis is presented in subsection 3.2.

3.1.1. Peak position versus concentration. Figure 4 shows the concentration dependence of the peak positions of the most intense Raman bands in different configurations. It appears

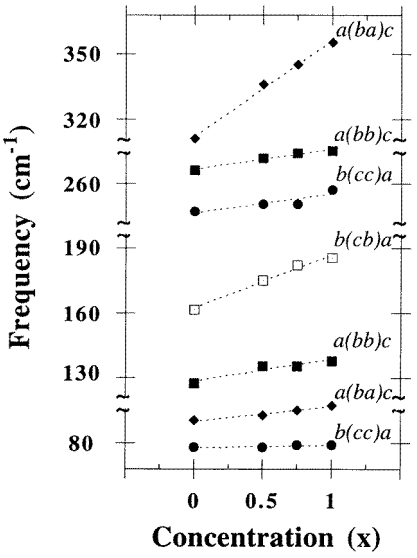

Figure 4. The concentration dependence of some peak positions in different configurations from $x = 0$ ($BaMnF_4$) to $x = 1$ ($BaZnF_4$). The dotted lines are guides for the eyes. Different frequency ranges have been separated.

that while most of the Raman frequencies just slightly increase from $BaMnF_4$ to $BaZnF_4$, a few of them display a strong shift. This is the case for the mode observed at 359 cm^{-1} $(a(ba)c)$ and at 181 cm^{-1} $(b(cb)a)$ for $BaZnF_4$.

It can be noted that the $BaMnF_4$ frequencies are smaller than the $BaZnF_4$ ones. This fact cannot be explained by the mass difference ($m_{Mn} = 54.9$ g $mol^{-1} < m_{Zn} = 65.4$ g mol^{-1}), but should be attributed to a weakening of the force constants. This results from the fact that the interatomic distances are larger in $BaMnF_4$ than in $BaZnF_4$ [1], a consequence of the differences of the ionic radii ($r_{Mn} = 0.83$ Å $> r_{Zn} = 0.74$ Å) [18].

3.2. Temperature evolution of the Raman spectra

The spectra obtained in the (a, b) scattering plane for different temperatures between 10 and 300 K for $BaMn_{0.5}Zn_{0.5}F_4$ ((cc) and (cb) polarizations), and $BaMn_{0.25}Zn_{0.75}F_4$ ((cc) and (ca) polarizations) are shown in figures 5 and 6.

The new lines observed at low temperatures appear as the result of a decreasing of the linewidths; the number of lines remains smaller than expected. No Raman signature for a structural phase transition is observed in this temperature range.

3.2.1. Linewidth versus concentration and temperature. The evolution of the linewidth versus temperature of the mode observed in the (cc) spectrum and located at 289 cm^{-1} in $BaMn_{0.5}Zn_{0.5}F_4$, at 293 cm^{-1} in $BaMn_{0.25}Zn_{0.75}F_4$, and at 294 cm^{-1} in $BaZnF_4$ is plotted in figure 7.

As usual, we observe that the introduction of Mn^{2+} in $BaZnF_4$ crystal acts on the value of the linewidth at lower temperature (Γ_0): in the concentration range investigated the greater the manganese concentration the larger the linewidth. This can be imputed to the fact that the chemical substitution for Zn^{2+} with Mn^{2+} in $BaZnF_4$ induces an increase of

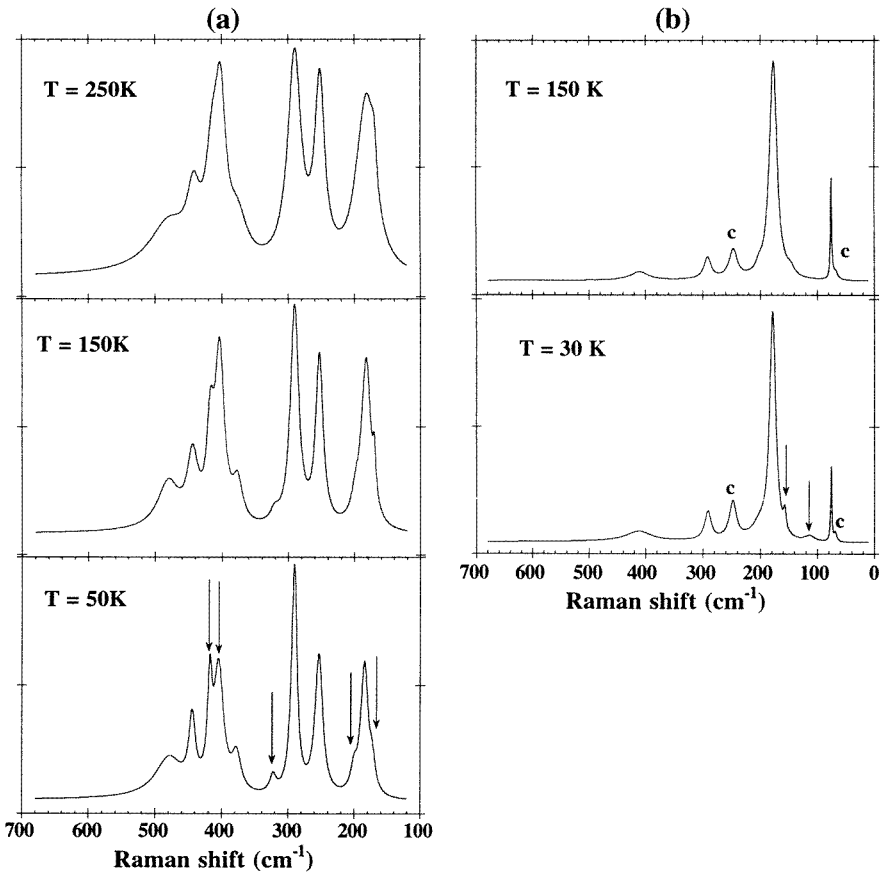

Figure 5. Raman spectra as a function of temperature for $BaMn_{0.5}Zn_{0.5}F_4$: (a) $b(cc)a$ and (b) $b(cb)a$. The arrows indicate the new lines observed at lower temperatures and c a possible contamination.

Table 3. Evolution of the linewidths Γ_0, and ΔW (see the text) as a function of the Mn^{2+} concentration $(1-x)$ in the solid solution $BaMn_{1-x}Zn_xF_4$: case of the line at 294 cm^{-1} for $BaZnF_4$.

$1-x$	0.5	0.25	0
ΔW (K)	314 ± 45	288 ± 30	257 ± 25
Γ_{300} (cm^{-1})	25 ± 1	24 ± 1	23 ± 1
Γ_0 (cm^{-1})	10 ± 1	7 ± 1	5 ± 1

the disorder which actually is already present in the pure salt.

Considering in addition the thermal disorder, it is convenient to analyse the linewidth using an appropriate expression [19]:

$$\Gamma = \Gamma_0 + A \exp\left(\frac{-\Delta W}{kT}\right) \tag{1}$$

where ΔW represents the activation energy of some relaxator. From a refinement it appears

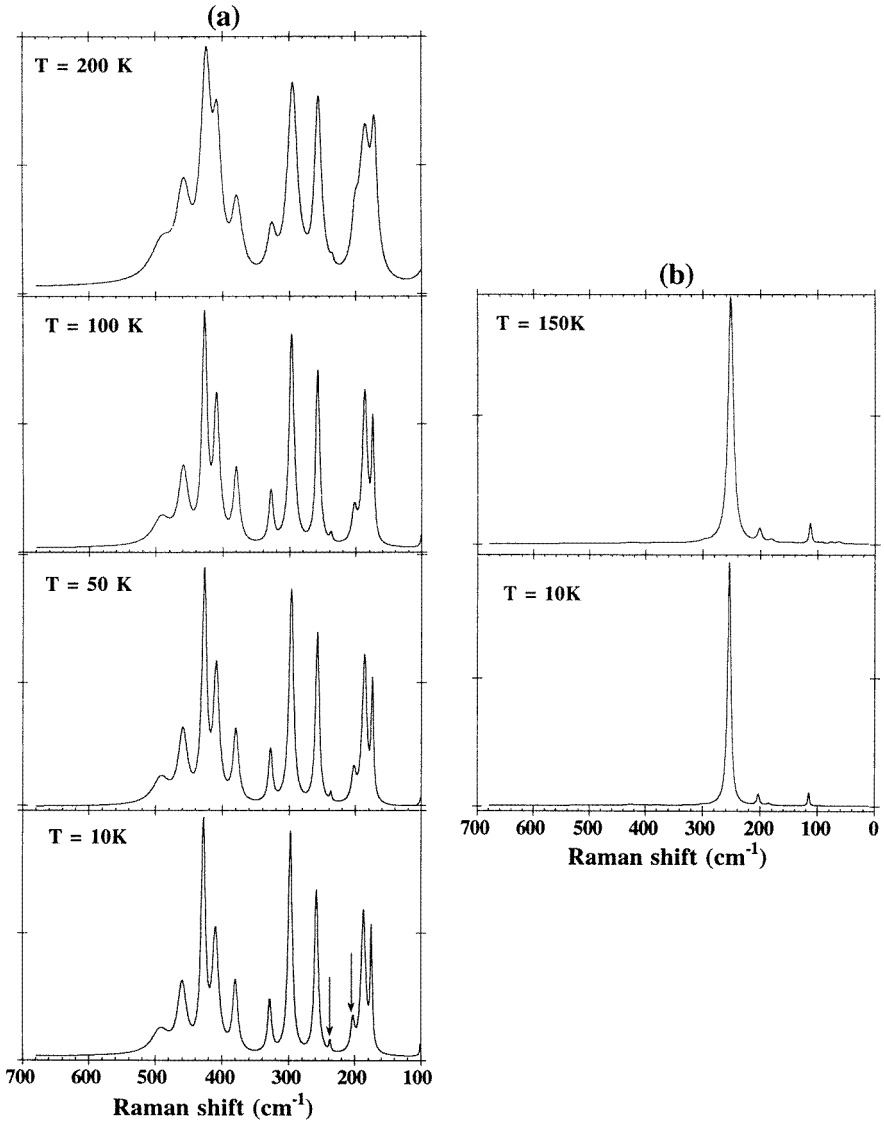

Figure 6. Raman spectra as a function of temperature for $BaMn_{0.25}Zn_{0.75}F_4$: (a) $a(cc)b$ and (b) $a(ca)b$. The arrows indicate the new lines observed at lower temperatures.

that the lines drawn in figure 7 can be described by relation (1). Table 3 gives the values of Γ_0 and ΔW calculated for the three compounds. The increasing of the Mn^{2+} concentration results in an increasing of the activation energy ΔW.

3.2.2. New weak lines at low frequency. In order to analyse the low-frequency signals several spectra were recorded in both the Stokes and anti-Stokes regions with an improved integration time, over the whole temperature range. Some of them are shown in figure 8 for different concentrations. It can be noted that as the temperature decreases the bands

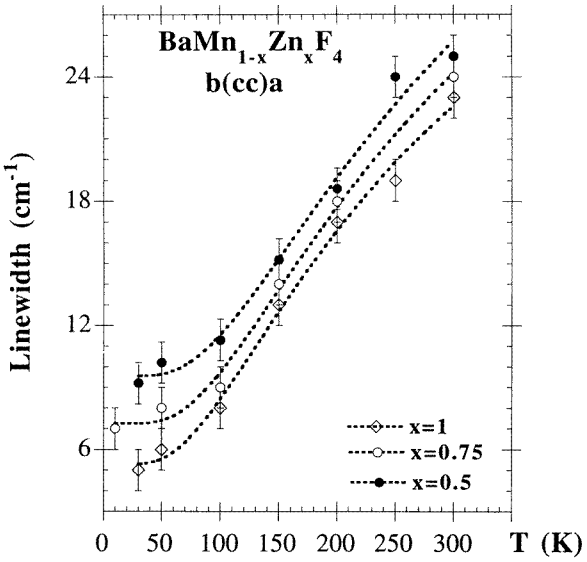

Figure 7. The temperature evolution of the linewidth of the mode (*cc*) located at 289 cm^{-1} for $BaMn_{0.5}Zn_{0.5}F_4$, at 293 cm^{-1} for $BaMn_{0.25}Zn_{0.75}F_4$, and at 294 cm^{-1} for $BaZnF_4$.

observed between 5 and 50 cm^{-1} undergo important variations, the rest of the spectra remaining almost unchanged. The characteristics, i.e. peak shifts, integrated intensities and half-widths, of the bands denoted as A and B in figure 8 have been analysed, and the temperature behaviour of the frequency is shown in figure 9 for $x = 0.5, 0.75$ and 1. In figure 9(c) the hatched region corresponds to the quasi-elastic response which spreads up to about 18 cm^{-1} [14]. The lower-frequency band (A), located at 26 cm^{-1} for $x = 0.5$ and at 16 cm^{-1} for $x = 0.75$ at low temperature, displays a softening behaviour with a minimum frequency at about 150 and 70 K, respectively. A hardening of this band can be noticed on approaching the lowest temperatures, particularly in the case where $x = 0.5$. The frequency of the other band (B) located at about 35 to 40 cm^{-1} is almost temperature independent.

As we were concerned with the intensity evolution of these lines, with regard to their weakness, we tried to normalize their integrated intensity with respect to several modes having a strong intensity and a 'standard' temperature behaviour (modes at 75, 290 and 410 cm^{-1}). The results were very similar whatever the reference was, so the evolutions shown in figures 10(a) for $x = 0.5$ and 10(b) for $x = 0.75$ can be considered as reliable. The width variations are also reported in figure 10.

In the solid solution $BaMn_{0.5}Zn_{0.5}F_4$, while the temperature decreases, the intensity of the A band increases, and that of the B band becomes very small. In view of this, we have examined the possibility of an interpretation of the unexpected B band in terms of a second-order Raman scattering process. Based on this assumption the temperature variation of the Stokes intensity would exhibit the so-called $(n + 1)^2$ dependence (where n represents the Bose–Einstein occupation factor for the phonons giving rise to such signals), as is shown by the continuous line in figure 10(a). In fact this interpretation does not reproduce the experimental results correctly, and the integrated intensities of the two bands seem to be correlated.

In the $BaMn_{0.25}Zn_{0.75}F_4$ solid solution the integrated intensity of the A band strongly

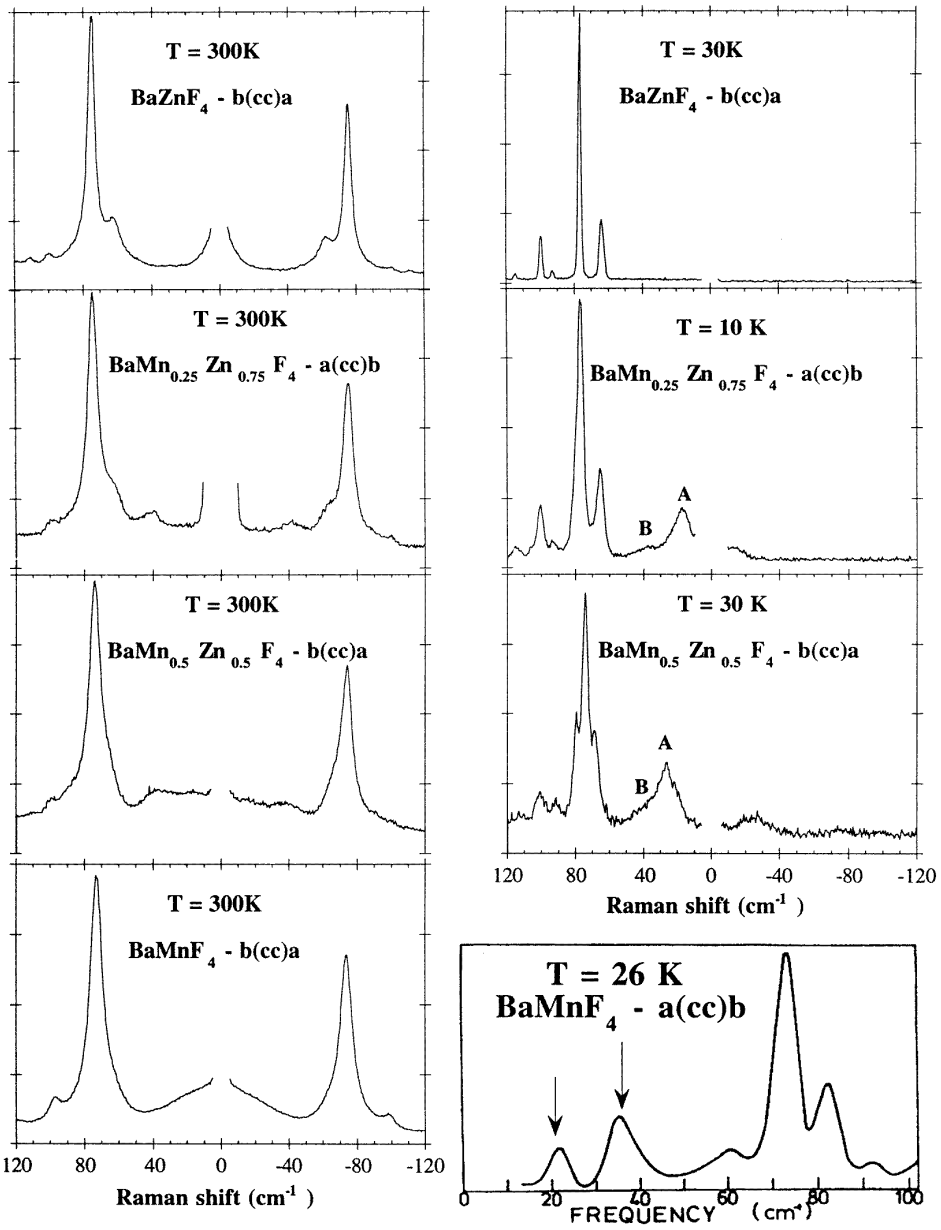

Figure 8. Raman spectra of $BaMn_{1-x}Zn_xF_4$ solid solution for $x = 0$ [21], 0.5, 0.75 and 1 at 300 and 30 K. Two new weak lines (A and B) are observed for both solid solutions at lower frequencies. Note that in this same spectral region, two modes (indicated by arrows) have also been observed in $BaMnF_4$ below the incommensurate transition [20].

increases at low temperature, while for the other mode it remains constant.

Finally, the widths of these bands for all concentrations increase with temperature, except that of the B band of $BaMn_{0.25}Zn_{0.75}F_4$, which remains at a constant value equal to 13 cm^{-1} over the whole temperature range.

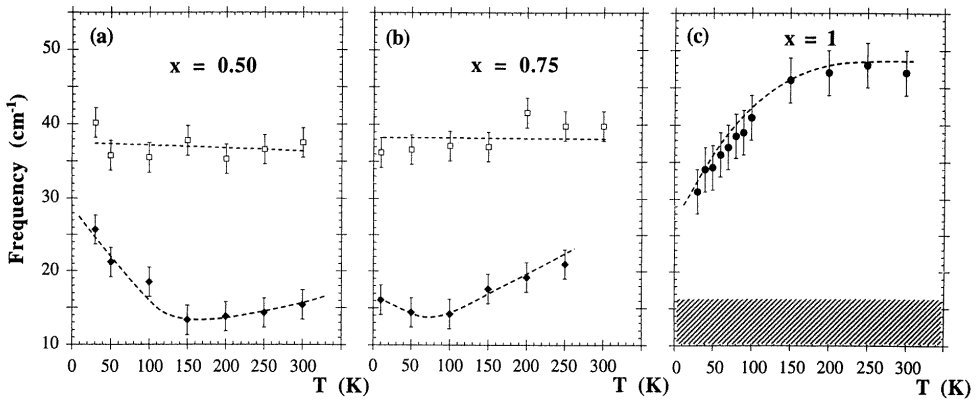

Figure 9. Frequency shifts of the lower bands. The full lozenges represent the A band and the open squares represent the B band in the case where $x = 0.5$ (a) and $x = 0.75$ (b). For the pure Zn compound ($x = 1$), the full circles represent a mode located at about 30 cm^{-1} at 30 K—not visible in figure 8—and the hatched region corresponds to the relaxator response (see [13, 14]).

4. Discussion

In this section we would like to discuss the low-frequency bands observed for the different compounds since they obviously contain information about the unusual behaviour of the $BaMF_4$.

As shown in figure 8 the $BaMnF_4$ low-temperature $a(cc)b$ spectrum displays two frequency bands at 21 and 36 cm^{-1}. This has been demonstrated by various authors [15, 17, 22].

Using a $c(bb)a$ geometry Lockwood *et al* [15] have studied their temperature dependence, but as the parameters (strength, damping and frequency) obtained from a two-coupled-modes model displayed a very unusual behaviour they could not conclude that they had observed the so-called amplitudon and/or phason modes. Nevertheless they assumed that the two modes are fluctuations induced by the incommensurate phase. Recently Tsuboi *et al* (see [21]) have made more detailed measurements of the same spectrum in the $a(cc)b$ geometry. They also interpreted the two bands as coupled modes because of their asymmetric shape and their frequency and intensity behaviour against temperature†. They considered that the mode located at 36 cm^{-1} represents the amplitudon, and the other one that appears in the new phase is 'new', and remains 'hard'. In both cases the two low-frequency bands are associated with the new incommensurate phase below T_i.

Considering now the case of $BaZnF_4$, recent neutron scattering measurements [23] of the low-frequency phonons display a soft branch at (0.5 0.5 0.5). As the frequency of the weak band observed by Raman spectroscopy for this compound (figure 9(c)) [13] is two times the frequency observed by neutron scattering at (0.5 0.5 0.5) and as their temperature behaviours are similar, the Raman band can be explained via a two-phonon process.

Taking into account all of these experimental observations, we are able to compare the temperature evolution of the low-frequency region in $BaMn_{1-x}Zn_xF_4$ solid solutions with that of $BaMnF_4$ and $BaZnF_4$. In each case there are two bands—one is 'hard' and the other

† Note that in the concentration range investigated here, due to the weakness of the A and B bands and their overlapping, it has not been possible to unambiguously demonstrate any asymmetry.

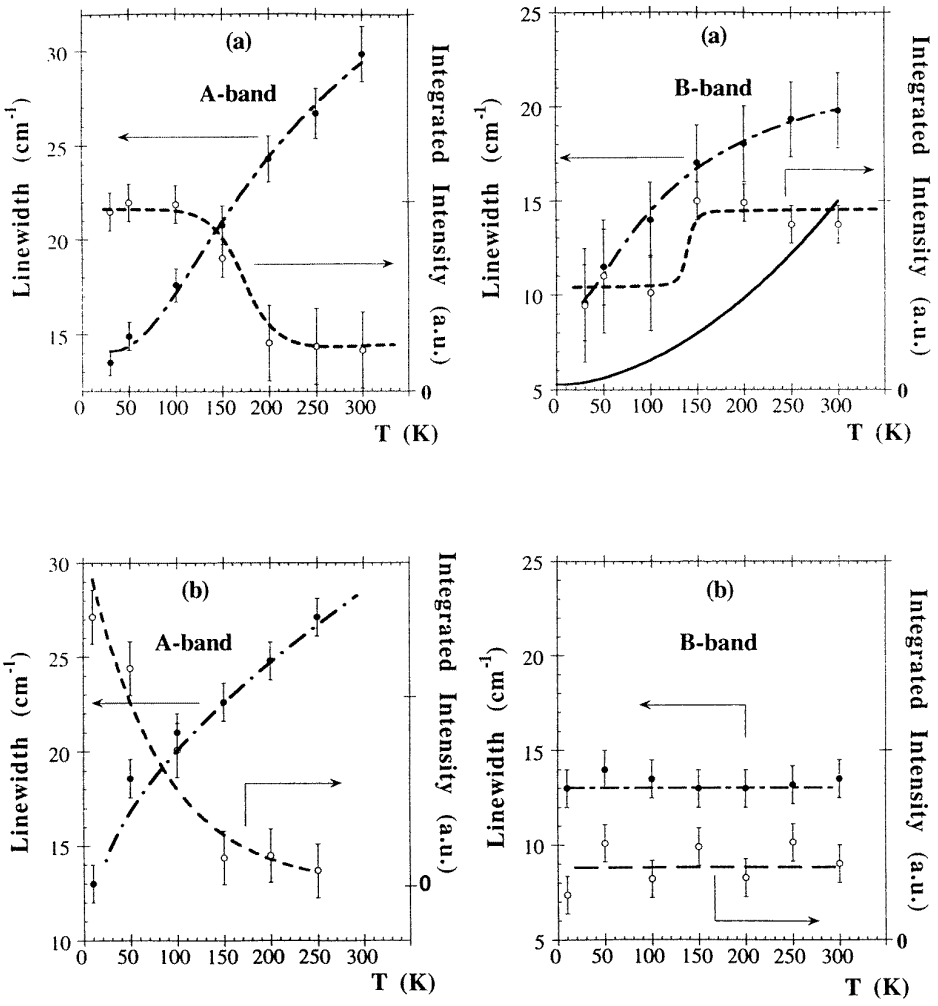

Figure 10. The linewidth (full circles) and integrated intensity (open circles) evolution against temperature for the lower bands A and B observed for $BaMn_{1-x}Zn_xF_4$: (a) $x = 0.5$ and (b) $x = 0.75$. In (a) the full line shows the temperature variation of a second-order Raman scattering process for a mode at $\omega \approx 38$ cm^{-1}. Note that the zero (0) of the intensity scale is indicated on the right-hand side [21].

is 'soft'. However, the evolution against temperature of the 'soft-mode' frequency is quite different. In $BaZnF_4$ the soft-mode frequency decreases at low temperature, whereas that in $BaMnF_4$ increases at low temperature.

Let us now consider our previous x-ray measurements [14], on the basis of which we concluded that 2D dynamical clusters in $BaZnF_4$, which can be considered as precursors of the $BaMnF_4$-type phase transition, were present. As the substitution for the Mn^{2+} ions with Zn^{2+} ions leads to the observation of an incommensurate phase in the solid solution $BaMn_{1-x}Zn_xF_4$, for $0 \leqslant x \leqslant 0.20$, we can argue that this substitution leads to an evolution of the 2D cluster behaviour. So it seems reasonable to think that the presence of these lower Raman bands can be associated with the existence of 2D clusters, whose size increases with

the amount $(1 - x)$ of Mn^{2+} ions. The decrease of the width and the increases of the intensity and frequency of the A band should be connected with an increase of the cluster sizes within a local order. The transition to an incommensurate phase will be possible when some long-range order is reached. This is not the case for the solid solutions investigated here. Nevertheless something occurs when the A-band frequency reaches a minimum, so the hypothesis that a glass transition occurs would not be unrealistic.

Of course the mechanism of the cluster evolution is not yet clear, and further experimental investigations must be done in order to check our hypothesis. The analysis of the inelastic neutron scattering data that have just been collected on $BaZnF_4$, including dynamical parameters, should help to explain the behaviour of these materials.

Acknowledgments

It is a pleasure for us to thank J L Sauvajol for helpful discussions, G Niesseron for the crystal growth, B Delettre for crystal polishing, and P Saint-Grégoire and M Lopez for calorimetric measurements. HNB is grateful to the Brazilian 'Conselho Nacional de Desenvolvimento Científico e Tecnológico—CNPq' for its financial support.

References

[1] Keve E T, Abrahams S C and Bernstein J L 1969 *J. Chem. Phys.* **51** 4928
[2] Lapasset J, Bordallo H N, Almairac R and Nouet J 1996 *Z. Kristallogr.* submitted
[3] Aizawa K and Ishiwara H 1993 *Appl. Phys. Lett.* **63** 1765
[4] Cox D E, Shapiro S M, Cowley R A, Eibschütz M and Guggenheim H J 1979 *Phys. Rev.* B **19** 5754
[5] Ryan T W 1986 *J. Phys. C: Solid State Phys.* **19** 1097
[6] Sciau P, Clin M, Rivera J P and Schmid H 1990 *Ferroelectrics* **105** 201
[7] Scott J F 1986 Statics and dynamics of incommensurate $BaMnF_4$ *Incommensurate Phase in Dielectrics* ed R Blinc and A P Levanyuk (Amsterdam: Elsevier)
[8] Barthès-Régis M, Almairac R, Saint-Grégoire P, Filippini C, Steigenberger U, Nouet J and Gesland Y 1983 *J. Physique Lett.* **44** L829
[9] Asahi T, Tomizawa M, Kobayashi J and Kleemann W 1992 *Phys. Rev.* B **45** 1971
[10] Scott J F 1979 *Rep. Prog. Phys.* **12** 1055
[11] Quilichini M and Poulet H 1974 *Phys. Status Solidi* b **62** 501
[12] Quilichini M, Ryan J F Scott J F and Guggenheim H J 1975 *Solid State Commun.* **16** 471
[13] Bordallo H N, Bulou A, Almairac R and Nouet J 1994 *J. Phys.: Condens. Matter* **6** 10 365
[14] Almairac R, Bordallo H N, Bulou A and Nouet J 1995 *Phys. Rev.* B **52** 9370
[15] Lockwood D J, Murray A F and Rowell N L 1981 *J. Phys. C: Solid State Phys.* **14** 753
[16] Tsuboi T 1989 *Phase Transitions* **18** 119
[17] Kamba S, Petzelt J and Zelezny V 1986 *Czech. J. Phys.* B **36** 848
[18] Shannon R D 1976 *Acta Crystallogr.* A **32** 751
[19] Poulet H and Mathieu J P 1970 *Spectres de Vibration et Symétrie des Cristaux* (New York: Gordon and Breach)
[20] Tsuboi T 1989 *J. Phys. Soc. Japan* **58** 2211
[21] In the interpretation of the additional mode located at about 48 cm^{-1} in [13], we have examined the possibility that this unexpected line could be attributed to a second-order Raman process. Meanwhile in figure 10(b) of [13]: (i) we did not report correctly the theoretical curve (the exact behaviour of a second-order Raman process is that shown in the figure 10 of the present paper); and (ii) we did not indicate precisely the zero (0) of the integrated intensity. However, these facts do not invalidate our inference that Stokes intensity does not strictly exhibit the so-called $(n + 1)^2$ dependence over the whole temperature range.
[22] Tsuboi T and Hangyo M 1989 *J. Phys. Soc. Japan* **58** 1887
[23] Bordallo H N, Almairac R, Bulou A, Nouet J and Currat R 1996 in preparation